PHYSICAL REVIEW C **92**, 055502 (2015)

Reexamining the light neutrino exchange mechanism of the $0\nu\beta\beta$ decay with left- and right-handed leptonic and hadronic currents

Dušan Štefánik,[1] Rastislav Dvornický,[1,2] Fedor Šimkovic,[1,3,4] and Petr Vogel[5]
[1]*Department of Nuclear Physics and Biophysics, Comenius University, Mlynská dolina F1, SK-842 48 Bratislava, Slovakia*
[2]*Dzhelepov Laboratory of Nuclear Problems, JINR, 141980 Dubna, Russia*
[3]*Bogoliubov Laboratory of Theoretical Physics, JINR, 141980 Dubna, Russia*
[4]*Czech Technical University in Prague, 128-00 Prague, Czech Republic*
[5]*Kellogg Radiation Laboratory, California Institute of Technology, Pasadena, California 91125, USA*
(Received 6 July 2015; published 4 November 2015)

The extension of the Majorana neutrino mass mechanism of the neutrinoless double-beta decay ($0\nu\beta\beta$) with the inclusion of right-handed leptonic and hadronic currents is revisited. While only the exchange of light neutrinos is assumed, the $s_{1/2}$ and $p_{1/2}$ states of emitted electrons as well as recoil corrections to the nucleon currents are taken into account. Within the standard approximations the decay rate is factorized into a sum of products of kinematical phase-space factors, nuclear matrix elements, and the fundamental parameters that characterize the lepton number violation. Unlike in the previous treatments, the induced pseudoscalar term of hadron current is included, resulting in additional nuclear matrix elements. An improved numerical computation of the phase-space factors is presented, based on the exact Dirac wave functions of the $s_{1/2}$ and $p_{1/2}$ electrons with finite nuclear size and electron screening taken into account. The dependence of values of these phase-space factors on the different approximation schemes used in evaluation of electron wave functions is discussed. The upper limits for effective neutrino mass and the parameters $\langle\lambda\rangle$ and $\langle\eta\rangle$ characterizing the right-handed current mechanism are deduced from data on the $0\nu\beta\beta$ decay of ^{76}Ge and ^{136}Xe using nuclear matrix elements calculated within the nuclear shell model and quasiparticle random phase approximation. The differential decay rates, i.e., the angular correlations and the single electron energy distributions for various combinations of the total lepton number violating parameters that can help to disentangle the possible mechanism, are described and discussed.

DOI: 10.1103/PhysRevC.92.055502 PACS number(s): 21.60.Jz, 23.40.Hc, 14.60.Pq

I. INTRODUCTION

The neutrinoless double-beta ($0\nu\beta\beta$) decay is a process in which an atomic nucleus with Z protons decays to another one with two more protons and the same mass number A, by emitting two electrons and nothing else:

$$(A,Z) \to (A,Z+2) + 2e^{-}. \tag{1}$$

Observing the $0\nu\beta\beta$ decay guarantees that neutrinos are massive Majorana particles; this means that the neutrino is identical to its own antiparticle [1]. $0\nu\beta\beta$ decay violates total lepton number conservation and is forbidden in the standard model.

When the light-neutrino exchange produced by left-handed currents is the driving mechanism for $0\nu\beta\beta$ decay, the relation between the effective Majorana neutrino mass and the inverse half-life of the $0\nu\beta\beta$ decay can be written as [2]

$$\left[T^{0\nu}_{1/2}\right]^{-1} = G^{0\nu}(Q,Z) g_A^4 |M^{0\nu}|^2 \frac{|m_{\beta\beta}|^2}{m_e^2}, \tag{2}$$

where $G^{0\nu}(Q,Z)$, g_A, and $M^{0\nu}$ represent the phase-space factor, the axial-vector coupling constant, and the nuclear matrix element of the process, respectively. In that case the ultimate goal of the search for $0\nu\beta\beta$ decay is the determination of the effective Majorana neutrino mass,

$$m_{\beta\beta} = U_{e1}^2 m_1 + U_{e2}^2 m_2 + U_{e3}^2 m_3. \tag{3}$$

Here, U_{ei} and m_i ($i = 1,2,3$) are elements of the Pontecorvo-Maki-Nakagawa-Sakata neutrino mixing matrix and masses of neutrinos, respectively.

An improved calculation of $G^{0\nu}$ in that case, taking into account the electron Dirac wave functions with finite nuclear size and electron screening, was performed in Ref. [3]. The main theoretical uncertainty is represented in the computed values of the nuclear matrix elements. There is a factor of 2–3 difference between the different methods of calculations of the $M^{0\nu}$.

The left-right symmetric theories [4,5] provide a natural framework to understand the origin of neutrino Majorana masses. In general one cannot predict the scale where the left-right symmetry is realized, but it is natural to assume that it is as low as $\sim$ a few TeV, which can affect the $0\nu\beta\beta$ decay rate significantly.

In the left-right symmetric theories, in addition to the left-handed $V-A$ weak currents also leptonic and hadronic right-handed $V+A$ weak currents are present. In that case a new mechanism of the $0\nu\beta\beta$ decay needs to be considered. In the past the $0\nu\beta\beta$ decay rate in the presence of the right-handed leptonic and hadronic currents was discussed in Refs. [6,7]. Recently, contributions to the $0\nu\beta\beta$ decay in TeV-scale left-right symmetric models for type-I seesaw dominance were revisited [8–11]. By making a qualitative analysis without considering relevant phase-space factors and nuclear matrix elements, it was found that W_L-W_R exchange (λ mechanism) and W_L-W_R mixing (η mechanism) could give a dominant contribution to the $0\nu\beta\beta$-decay amplitude by assuming a wide particle physics available parameter space including left-right

neutrino mixing [10,11]. We note that the discovery of a nonstandard $0\nu\beta\beta$-decay mechanism such as a right-handed current would rule out most models of baryogenesis at scales above 40 TeV [12].

The goal of this paper is to revisit the $0\nu\beta\beta$-decay mechanism due to the right-handed currents by considering an exact Dirac wave function of electrons and the higher order terms of nucleon current. We note that in Ref. [6] the effect of an induced pseudoscalar term of nucleon current was neglected and phase space factors were expressed using approximate electron wave functions for a uniform charge distribution in a nucleus by keeping only the lowest terms in the power expansion in r. In that context the subject of interest is the comparison of the power expansion versus the exact treatment and the finite nuclear size effects. In this work the newly derived decay rate will be written in a compact form and the corresponding nuclear matrix elements will be presented by assuming the usual closure approximation for intermediate nuclear states. The phase-space factors will be evaluated by using the exact Dirac wave functions with finite nuclear size and electron screening. The differential characteristics, i.e., the angular correlations and the single-electron energy distributions will be described and discussed, and the decay rates and updated constraints on the lepton number violating parameters for different combinations of the total lepton number violating parameters will be recalculated. This will make it possible to judge the importance of the λ and η mechanism.

II. ELECTRON WAVE FUNCTIONS

An important ingredient in the calculation of the electron energy spectrum is the radial electron wave function distorted by the Coulomb field. We adopt the Dirac wave functions in a central field,

$$\Psi(\varepsilon,\boldsymbol{r}) = \sum_{\kappa\mu} \begin{pmatrix} g_\kappa(\varepsilon,r)\chi_{\kappa\mu}(\hat{r}) \\ i f_\kappa(\varepsilon,r)\chi_{-\kappa\mu}(\hat{r}) \end{pmatrix}, \tag{4}$$

given, e.g., by Rose [13]. Here, ε and $\boldsymbol{r}$ stand for energy and position vector of the electron, respectively, $r = |\boldsymbol{r}|$ and $\hat{r} = \boldsymbol{r}/r$. The index κ takes positive and negative integer values ($\kappa = \pm k, k = 1,2,3,\dots$). Total angular momentum is given as $j_\kappa = |\kappa| - 1/2$ while orbital angular momentum takes values

$$l_\kappa = \begin{cases} |\kappa| - 1 & \text{for } \kappa < 0, \\ \kappa & \text{for } \kappa > 0. \end{cases} \tag{5}$$

Radial wave functions $g_\kappa(\varepsilon,r)$ and $f_\kappa(\varepsilon,r)$ obey the radial Dirac equations,

$$\begin{aligned} \frac{dg_\kappa}{dr} &= -\frac{\kappa+1}{r} g_\kappa + (\varepsilon - V(r) + m_e) f_\kappa, \\ \frac{df_\kappa}{dr} &= -(\varepsilon - V(r) - m_e) g_\kappa + \frac{\kappa-1}{r} f_\kappa, \end{aligned} \tag{6}$$

where $V(r)$ is the central Coulomb potential. The natural units $\hbar = c = 1$ are used.

The electron wave function expressed in terms of spherical waves is given by

$$\Psi(\varepsilon,\boldsymbol{r}) = \Psi^{(s_{1/2})}(\varepsilon,\boldsymbol{r}) + \Psi^{(p_{1/2})}(\varepsilon,\boldsymbol{r}) + \cdots . \tag{7}$$

Here, the superscript displays the orbital angular momentum ($l_\kappa = 0,1,2,\dots$) in a spectroscopic notation ($l_\kappa = s,p,d,\dots$) and the total angular momentum j_κ. The states of particular interest in our calculations are

$$\begin{aligned} \Psi^{(s_{1/2})}(\varepsilon,\boldsymbol{r}) &= \begin{pmatrix} g_{-1}(\varepsilon,r)\chi_s \\ f_{+1}(\varepsilon,r)(\sigma\cdot\hat{\mathbf{p}})\chi_s \end{pmatrix}, \\ \Psi^{(p_{1/2})}(\varepsilon,\boldsymbol{r}) &= i\begin{pmatrix} g_{+1}(\varepsilon,r)(\sigma\cdot\hat{\mathbf{r}})(\sigma\cdot\hat{\mathbf{p}})\chi_s \\ -f_{-1}(\varepsilon,r)(\sigma\cdot\hat{\mathbf{r}})\chi_s \end{pmatrix}, \end{aligned} \tag{8}$$

where $\hat{p} = \boldsymbol{p}/p$ and p is the electron momentum. The asymptotic behavior of the radial wave functions for large values of pr is given by

$$\begin{aligned} &\begin{pmatrix} g_\kappa(\varepsilon,r) \\ f_\kappa(\varepsilon,r) \end{pmatrix} \\ &\approx \frac{1}{pr}\begin{pmatrix} \sqrt{\frac{\varepsilon+m_e}{2\varepsilon}}\sin\left(pr - l\frac{\pi}{2} + \delta_k + \alpha Z_f \frac{\varepsilon}{p}\ln 2pr\right) \\ \sqrt{\frac{\varepsilon-m_e}{2\varepsilon}}\cos\left(pr - l\frac{\pi}{2} + \delta_k + \alpha Z_f \frac{\varepsilon}{p}\ln 2pr\right) \end{pmatrix}. \end{aligned} \tag{9}$$

Z_f is the charge of the final system which generates the potential $V(r)$.

In what follows, different approximation schemes for the calculation of radial wave functions $g_{\pm1}$ and $f_{\pm1}$ associated with emitted electrons in the $s_{1/2}$ and $p_{1/2}$ wave states are briefly presented.

The approximation scheme A. The relativistic electron wave function in a uniform charge distribution in the nucleus is considered. The lowest terms in the power expansion in r are taken into account. The radial wave functions take the form

$$\begin{aligned} \begin{pmatrix} g_{-1}(\varepsilon,r) \\ f_{+1}(\varepsilon,r) \end{pmatrix} &\approx \sqrt{F_0(Z_f,\varepsilon)}\begin{pmatrix} \sqrt{\frac{\varepsilon+m_e}{2\varepsilon}} \\ \sqrt{\frac{\varepsilon-m_e}{2\varepsilon}} \end{pmatrix}, \\ \begin{pmatrix} g_{+1}(\varepsilon,r) \\ f_{-1}(\varepsilon,r) \end{pmatrix} &\approx \sqrt{F_0(Z_f,\varepsilon)} \\ &\quad\times \begin{pmatrix} \sqrt{\frac{\varepsilon-m_e}{2\varepsilon}}[\alpha Z_f/2 + (\varepsilon+m_e)r/3] \\ -\sqrt{\frac{\varepsilon+m_e}{2\varepsilon}}[\alpha Z_f/2 + (\varepsilon-m_e)r/3] \end{pmatrix}. \end{aligned} \tag{10}$$

Here, F_{k-1} (for $k = 1,2,\dots$) is given by

$$F_{k-1} = \left[\frac{\Gamma(2k+1)}{\Gamma(k)\Gamma(1+2\gamma_k)}\right]^2 (2pr)^{2(\gamma_k-k)} e^{\pi y}\Gamma(\gamma_k + iy)\,|^2\,, \tag{11}$$

where

$$\begin{aligned} \gamma_k &= \sqrt{k^2 - (\alpha Z_f)^2} \\ y &= \alpha Z_f \frac{\varepsilon}{p}. \end{aligned} \tag{12}$$

This approximation scheme was commonly used in the past calculations of the phase-space integrals of double-beta decay processes [6].

The approximation scheme B. The analytical solution of the Dirac equation for the pointlike nucleus is considered [14].

Radial wave functions then take the form

$$g_\kappa(\varepsilon,r) = \frac{\kappa}{k}\frac{1}{pr}\sqrt{\frac{\varepsilon+m_e}{2\varepsilon}}\frac{|\Gamma(1+\gamma_k+iy)|}{\Gamma(1+2\gamma_k)}(2pr)^{\gamma_k}e^{\pi y/2} \times \mathrm{Im}\{e^{i(pr+\xi)}\,{}_1F_1(\gamma_k-iy,1+2\gamma_k,-2ipr)\},$$

$$f_\kappa(\varepsilon,r) = \frac{\kappa}{k}\frac{1}{pr}\sqrt{\frac{\varepsilon-m_e}{2\varepsilon}}\frac{|\Gamma(1+\gamma_k+iy)|}{\Gamma(1+2\gamma_k)}(2pr)^{\gamma_k}e^{\pi y/2} \times \mathrm{Re}\{e^{i(pr+\xi)}\,{}_1F_1(\gamma_k-iy,1+2\gamma_k,-2ipr)\}, \quad (13)$$

with

$$e^{-2i\xi} = \frac{\gamma_k - iy}{\kappa - iym_e/\varepsilon}. \quad (14)$$

Here, ${}_1F_1(a,b,z)$ is the confluent hypergeometric function.

The approximation scheme C. The exact Dirac wave functions with finite nuclear size, which is taken into account by a uniform charge distribution in a sphere of nuclear radius R, are assumed [3]. The numerical calculation can be accomplished by the subroutine package RADIAL [15], where the input central potential is given by

$$V(r) = \begin{cases} -\frac{\alpha Z_f}{2R}\left(3-\left(\frac{r}{R}\right)^2\right) & \text{for } r \leqslant R, \\ -\frac{\alpha Z_f}{r} & \text{for } r > R. \end{cases} \quad (15)$$

Here, $R = r_0 A^{1/3}$ with $r_0 = 1.2$ fm. In the code the radial Dirac equations are solved by using piecewise exact power series expansion, which is summed up to a prescribed accuracy so that truncation errors can be avoided completely.

The approximation scheme D. The exact Dirac wave functions with finite nuclear size and electron screening are used [3]. The effect of screening of atomic electrons is taken into account by the Thomas-Fermi approximation. It uses the solution of the Thomas-Fermi equation,

$$\frac{d^2\varphi}{dx^2} = \frac{\varphi^{3/2}}{\sqrt{x}}, \quad (16)$$

with $x = r/b$, where

$$b = \frac{1}{2}\left(\frac{3\pi}{4}\right)^{2/3} a_0 Z_f^{-1/3}. \quad (17)$$

The Thomas-Fermi function can be rewritten in terms of an effective charge $\varphi(x) = Z_{\mathrm{eff}}(x)/Z_f$. Therefore, boundary conditions

$$\varphi(0) = 1, \quad \varphi(\infty) = \frac{2}{Z_f} \quad (18)$$

of Eq. (16) take into account the fact that the final atom is a positive ion with electric charge +2. We adopt here the Majorana method described in Ref. [16] in order to solve Eq. (16). The input potential is then $V(r) = \varphi(r)V_0(r)$, where $V_0(r)$ is defined in Eq. (15).

In Fig. 1 radial wave functions of an electron in the $s_{1/2}$ wave state [$g_{-1}(\varepsilon)$ and $f_{+1}(\varepsilon)$] and in the $p_{1/2}$ wave state [$g_{+1}(\varepsilon)$ and $f_{-1}(\varepsilon)$] evaluated at $r = R$ are plotted as a function of the electron kinetic energy $\varepsilon - m_e$ for the case of the double-β decay of ^{150}Nd. We see that wave functions A, which correspond to leading finite-size Coulomb, agree qualitatively well with wave functions of the other approaches in the case of $g_{-1}(\varepsilon)$ and $f_{-1}(\varepsilon)$ but that there are significant differences for $g_{+1}(\varepsilon)$ and $f_{+1}(\varepsilon)$. These differences are apparent especially at lower energies. We notice also a rather good agreement between results for wave functions of B and C in general. The screening of atomic electrons affects mostly the $p_{1/2}$ wave functions, but is essentially negligible for the $s_{1/2}$ states.

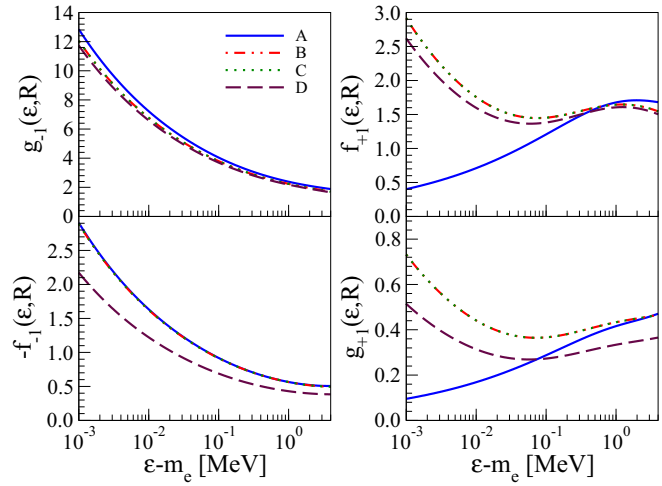

FIG. 1. (Color online) The radial wave functions of an electron in the $s_{1/2}$ wave state, $g_{-1}(\varepsilon)$ and $f_{+1}(\varepsilon)$ (upper panels), and in the $p_{1/2}$ wave state, $g_{+1}(\varepsilon)$ and $f_{-1}(\varepsilon)$ (lower panels), as function of the electron kinetic energy $\varepsilon - m_e$. Results are presented for an electron emitted in the double-β decay of ^{150}Nd. In an evaluation of radial wave functions (w.f.) four different approximation schemes are considered [see Sec. (II) for details]: (A) the standard approximation of Doi *et al.* [6]. (B) An analytical solution of Dirac equations assuming a pointlike nucleus. (C) An exact solution of Dirac equations for a uniform charge distribution in the nucleus, considered at the nuclear surface. (D) The same as the preceding case but the electron screening is taken into account [3].

III. DECAY RATE FOR THE NEUTRINOLESS DOUBLE-BETA DECAY

One of the most prominent new physics model that incorporates the lepton number violation (LNV) and which leads to potentially observable rates for the $0\nu\beta\beta$ decay is the minimal left-right symmetric model (LRSM) [4,5] which extends the standard model gauge symmetry to the group $\mathrm{SU}(2)_L \otimes \mathrm{SU}(2)_R \otimes \mathrm{U}(1)_{B-L}$. The right-handed neutrinos necessary appear here as a part of the $\mathrm{SU}(2)_R$ doublets. The lepton multiplets $L_i = (\nu_i, l_i)$ are characterized by the quantum numbers $Q_{L_L} = (1/2, 0, -1)$ and $Q_{L_R} = (0, 1/2, -1)$ under $\mathrm{SU}(2)_L \otimes \mathrm{SU}(2)_R \otimes \mathrm{U}(1)_{B-L}$. The Higgs sector contains a bidoublet ϕ and two triplets Δ_L and Δ_R with vacuum expectation values (VEVs) v_L and v_R, respectively. The VEVs fulfill the condition $v_L v_R = v^2$. The VEV v_R breaks $\mathrm{SU}(2)_R \otimes \mathrm{U}(1)_{B-L}$ to $\mathrm{U}(1)_Y$ and generates masses for the right-handed W_R and Z_R gauge bosons and the heavy neutrinos. The W_L and W_R are in general not mass eigenstates and are related to the mass eigenstates W_1 and W_2 with masses M_1 and M_2

$(M_1 < M_2)$ as

$$\begin{pmatrix} W_L^- \\ W_R^- \end{pmatrix} = \begin{pmatrix} \cos\zeta & \sin\zeta \\ -\sin\zeta & \cos\zeta \end{pmatrix} \begin{pmatrix} W_1^- \\ W_2^- \end{pmatrix}. \tag{19}$$

Then, the effective current-current interaction which can trigger the $0\nu\beta\beta$ decay can be written as [6]

$$H^\beta = \frac{G_\beta}{\sqrt{2}} \left[j_L^\rho J_{L\rho}^\dagger + \chi j_L^\rho J_{R\rho}^\dagger + \eta j_R^\rho J_{L\rho}^\dagger + \lambda j_R^\rho J_{R\rho}^\dagger + \text{H.c.} \right]. \tag{20}$$

Here, $G_\beta = G_F \cos\theta_C$, where G_F and θ_C are the Fermi constant and Cabbibo angle, respectively. The coupling constants λ, η, and χ are chosen to be real. We have

$$\eta \simeq -\tan\zeta, \quad \chi = \eta, \quad \lambda \simeq \left(M_{W_1} / M_{W_2} \right)^2. \tag{21}$$

The left- and right-handed leptonic currents are given by

$$j_L^\rho = \bar{e}\gamma_\rho(1-\gamma_5)\nu_{eL}, \quad j_R^\rho = \bar{e}\gamma_\rho(1+\gamma_5)\nu_{eR}. \tag{22}$$

The ν_{eL} and ν_{eR} are the weak eigenstate electron neutrinos, which are expressed as superpositions of the light and heavy mass eigenstate Majorana neutrinos ν_j and N_j, respectively. The electron neutrinos eigenstates can be expressed as

$$\begin{aligned} \nu_{eL} &= \sum_{j=1}^{3} (U_{ej}\nu_{jL} + S_{ej}(N_{jR})^C), \\ \nu_{eR} &= \sum_{j=1}^{3} (T_{ej}^*(\nu_{jL})^C + V_{ej}^* N_{jR}). \end{aligned} \tag{23}$$

The $(3+3)$ scenario is assumed. The 3×3 block matrices in flavor space U, S, T, V, generalizations of the Pontecorvo-Maki-Nakagawa-Sakata matrix, constitute the 6×6 unitary neutrino mixing matrix [17]

$$\mathcal{U} = \begin{pmatrix} U & S \\ T & V \end{pmatrix}, \tag{24}$$

which diagonalizes the general 6×6 neutrino mass matrix in the basis $(\nu_L, (N_R)^C)^T$:

$$\mathcal{M} = \begin{pmatrix} M_L & M_D \\ M_D^T & M_R \end{pmatrix} \tag{25}$$

with Majorana and Dirac mass terms, which are proportional to $M_L \approx y_M v_L$, $M_R \approx y_M v_R$, and $M_D \approx y_D v$, where y_M and y_D are the Yukawa couplings. The full parametrization of matrix $\mathcal{U}$ includes 15 rotational angles and 10 Dirac and 5 Majorana CP violating phases. It is possible to decompose $\mathcal{U}$ as follows [17]:

$$\mathcal{U} = \begin{pmatrix} \mathbf{1} & \mathbf{0} \\ \mathbf{0} & U_0 \end{pmatrix} \begin{pmatrix} A & R \\ S & B \end{pmatrix} \begin{pmatrix} V_0 & \mathbf{0} \\ \mathbf{0} & \mathbf{1} \end{pmatrix}, \tag{26}$$

where $\mathbf{0}$ and $\mathbf{1}$ are the 3×3 zero and identity matrices, respectively. The parametrization of matrices A, B, R, and S and the corresponding orthogonality relations are given in [17]. In the limit case $A = \mathbf{1}$, $B = \mathbf{1}$, $R = \mathbf{0}$, and $S = \mathbf{0}$ there would be a separate mixing of heavy and light neutrinos, which would participate only in left- and right-handed currents, respectively. In that case only the neutrino mass mechanism of the $0\nu\beta\beta$ decay would be allowed and exchange neutrino momentum dependent mechanisms associated with the W_L-W_R exchange and W_L-W_R mixing would be forbidden. If masses of heavy neutrinos are above the TeV scale, the mixing angles responsible for mixing of light and heavy neutrinos are small. By neglecting the mixing between different generations of light and heavy neutrinos, the A, B, R, and S matrices can be approximated as follows:

$$A \approx \mathbf{1}, \quad B \approx \mathbf{1}, \quad R \approx \frac{m_D}{m_{\text{LNV}}}\mathbf{1}, \quad S \approx -\frac{m_D}{m_{\text{LNV}}}\mathbf{1}. \tag{27}$$

Here, m_D represents the energy scale of charged leptons and m_{LNV} is the total lepton number violating scale, which corresponds to masses of heavy neutrinos. For the sake of simplicity the same mixing angle is assumed for each generation of mixing of light and heavy neutrinos. We see that U_0 can be identified to a good approximation with the Pontecorvo-Maki-Nakagawa-Sakata (PMNS) matrix and V_0 is its analog for the heavy neutrino sector. Since V_0 is unknown, it is common to assume that the structure of V_0 is the same one as U_0.

Assuming the nonrelativistic impulse approximation, the left and right hadronic currents $J_L^{\rho\dagger}$ and $J_R^{\rho\dagger}$ become [6]

$$\begin{aligned} J_L^{\rho\dagger}(\mathbf{x}) = \sum_n \tau_n^+ \delta(\mathbf{x}-\mathbf{r}_n) \Bigg[& (g_V - g_A C_n) g^{\rho 0} \\ & + g^{\rho k} \left(g_A \sigma_n^k - g_V D_n^k - g_P q_n^k \frac{\vec{\sigma}_n \cdot \mathbf{q}_n}{2m_N} \right) \Bigg], \\ J_R^{\rho\dagger}(\mathbf{x}) = \sum_n \tau_n^+ \delta(\mathbf{x}-\mathbf{r}_n) \Bigg[& (g'_V + g'_A C_n) g^{\rho 0} \\ & + g^{\rho k} \left(-g'_A \sigma_n^k - g'_V D_n^k + g'_P q_n^k \frac{\vec{\sigma}_n \cdot \mathbf{q}_n}{2m_N} \right) \Bigg]. \end{aligned} \tag{28}$$

Here, $\mathbf{q}_n = \mathbf{p}_n - \mathbf{p}'_n$ is the momentum transfer between the nucleons. The final proton (initial neutron) possesses energy E'_n (E_n) and momentum $\mathbf{p}'_n$ $(\mathbf{p}_n)$. $\vec{\sigma}_n$, τ_n^+, and $\mathbf{r}_n$ are the Pauli matrix, the isospin raising operator, and the position operator, respectively. These operators act on the nth nucleon.

The nucleon recoil operators C_n and $\mathbf{D}_n$ are given by

$$\begin{aligned} C_n &= \frac{\vec{\sigma}\cdot(\mathbf{p}_n + \mathbf{p}'_n)}{2m_N} - \frac{g_P}{g_A}(E_n - E'_n)\frac{\vec{\sigma}\cdot\mathbf{q}_n}{2m_N}, \\ \mathbf{D}_n &= \frac{(\mathbf{p}_n + \mathbf{p}'_n)}{2m_N} - i\left(1 + \frac{g_M}{g_V}\right)\frac{\vec{\sigma}\times\mathbf{q}_n}{2m_N}. \end{aligned} \tag{29}$$

Here, m_N is the nucleon mass. $q_V \equiv q_V(q^2)$, $q_M \equiv q_M(q^2)$, $q_A \equiv q_A(q^2)$, and $q_P \equiv q_P(q^2)$ are, respectively, the vector, weak-magnetism, axial-vector, and induced pseudoscalar form factors in the case of left-handed hadronic currents. As the strong and electromagnetic interactions conserve parity there are relations among form factors entering the left-handed and right-handed hadronic currents [6]:

$$\frac{g_A}{g_V} = \frac{g'_A}{g'_V}, \quad \frac{g_M}{g_V} = \frac{g'_M}{g'_V}, \quad \frac{g_P}{g_V} = \frac{g'_P}{g'_V}. \tag{30}$$

We note that the induced pseudoscalar term of the space component of hadronic currents was not taken into account in derivation of the $0\nu\beta\beta$-decay rate presented in Ref. [6]. This simplification is avoided here.

Due to helicity matching of the propagating neutrino the decay amplitude can be divided into two parts:

(a) If both vertices are $V-A$ or $V+A$, the amplitude of the process is proportional to the neutrino mass m_j. We shall denote the corresponding parts of the $0\nu\beta\beta$-decay amplitude L-L and R-R terms, respectively.
(b) If one vertex is $V-A$ and the other is $V+A$, the four-momentum of propagating neutrino $q^\mu=(\omega,\mathbf{q})$ contributes. The corresponding part of the amplitude, which is denoted as L-R, is further separated into two terms, the ω term and the $\mathbf{q}$ term.

In the case of L-L and R-R terms the dominant contribution is associated with the emission of electrons in the $s_{1/2}$-wave state [18]. However, the $\mathbf{q}$ term changes the parity and therefore it requires that one of the final electrons be in the $s_{1/2}$ wave while the other must be in the $p_{1/2}$ wave, or both electrons must be in the $s_{1/2}$ wave and the nucleon recoil operator is taken into account. Nevertheless, the $\mathbf{q}$ term is not negligible since the ω term is suppressed by a factor $\varepsilon_{12}/q\approx 1/40$ [6], that makes the $\mathbf{q}$ term comparable or even larger in comparison with the ω term.

The standard approximations of Ref. [6] are adopted:

(i) Only mechanisms with the exchange of light neutrinos are considered and contributions from heavier neutrinos are neglected. Recently, it was concluded in Refs. [10,11] that mechanisms with the exchange of light neutrinos could give dominant contributions to the $0\nu\beta\beta$ amplitude in a wide range of the LRSM parameter space.
(ii) Closure approximation. Within this approximation energies of intermediate nuclear states $E_n-(E_i+E_f)/2$ are replaced by an average of $\bar{E}_n-(E_i+E_f)/2\sim 10$ MeV and the sum over intermediate states is taken by closure, $\sum_n|n\rangle\langle n|=1$.
(iii) The R-R-part of the amplitude, that is multiplied by factor $|\lambda^2\sum_j m_j T^{*2}_{ej}|$, becomes negligible in comparison with $m_{\beta\beta}$. Thus it is neglected.
(iv) The terms proportional to the square of the nucleon recoil operators are also neglected.
(v) For the L-L part of the amplitude only electrons in the $s_{1/2}$ wave state are included. The inclusion of the $p_{1/2}$ electrons leads only to negligible contribution to the $0\nu\beta\beta$ standard decay rate [18].
(vi) In the case of the L-R term, two-nucleon potentials associated with the spatial q and time ω components of neutrino exchange potentials are simplified as follows:

$$H^l_q(\mathbf{x})=\int\frac{d\mathbf{q}}{2\pi^2}\left(\frac{q^l}{q+\Delta-\varepsilon_{12}}+\frac{q^l}{q+\Delta+\varepsilon_{12}}\right)e^{i\mathbf{q}\cdot\mathbf{x}}\approx\int\frac{d\mathbf{q}}{\pi^2 q}\frac{q^l}{q+\Delta}e^{i\mathbf{q}\cdot\mathbf{x}},$$

$$H_\omega(\mathbf{x})=\int\frac{d\mathbf{q}}{2\pi^2}\left(\frac{1}{q+\Delta-\varepsilon_{12}}-\frac{1}{q+\Delta+\varepsilon_{12}}\right)e^{i\mathbf{q}\cdot\mathbf{x}}\approx\varepsilon_{12}\int\frac{d\mathbf{q}}{\pi^2}\frac{1}{(q+\Delta)^2}e^{i\mathbf{q}\cdot\mathbf{x}},\tag{31}$$

where $\Delta=\bar{E}_n-(E_i+E_f)/2$ and $\varepsilon_{12}=\varepsilon_1-\varepsilon_2$. Here ε_1 and ε_2 represent the energies of the final electrons. Furthermore, contribution of the $p_{1/2}$-wave electrons and terms in which the nucleon recoil is multiplied by the small ω term are also neglected.
(vii) Since $|\chi U_{ej}g'_V/g_V|\ll|U_{ej}|$, the coupling constant χ in Hamiltonian (20) is neglected.
(viii) A factorization of phase-space factors and nuclear matrix elements is achieved by the approximation in which electron wave functions $g_{\pm1}(\varepsilon,r)$, $f_{\pm1}(\varepsilon,r)$ are replaced by their values at the nuclear radius R. The notation

$$g_{\pm1}(\varepsilon)\equiv g_{\pm1}(\varepsilon,R),\quad f_{\pm1}(\varepsilon)\equiv f_{\pm1}(\varepsilon,R)\tag{32}$$

is used.

Within the above approximations the $0\nu\beta\beta$-decay half-life can be written as

$$\begin{aligned}\left[T^{0\nu}_{1/2}\right]^{-1}&=\frac{\Gamma^{0\nu}}{\ln 2}\\&=g_A^4|M_{GT}|^2\left\{C_{mm}\left(\frac{|m_{\beta\beta}|}{m_e}\right)^2+C_{m\lambda}\frac{|m_{\beta\beta}|}{m_e}\langle\lambda\rangle\cos\psi_1\right.\\&\quad+C_{m\eta}\frac{|m_{\beta\beta}|}{m_e}\langle\eta\rangle\cos\psi_2+C_{\lambda\lambda}\langle\lambda\rangle^2+C_{\eta\eta}\langle\eta\rangle^2\\&\quad\left.+C_{\lambda\eta}\langle\lambda\rangle\langle\eta\rangle\cos(\psi_1-\psi_2)\right\}.\end{aligned}\tag{33}$$

The effective lepton number violating parameters associated with right-handed currents and their relative phases are given by

$$\begin{aligned}\langle\lambda\rangle&=\lambda\left|\sum_{j=1}^3 U_{ej}T^*_{ej}(g'_V/g_V)\right|,\\\langle\eta\rangle&=\eta\left|\sum_{j=1}^3 U_{ej}T^*_{ej}\right|,\\\psi_1&=\arg\left[\left(\sum_{j=1}^3 m_jU^2_{ej}\right)\left(\sum_{j=1}^3 U_{ej}T^*_{ej}(g'_V/g_V)\right)^*\right],\\\psi_2&=\arg\left[\left(\sum_{j=1}^3 m_jU^2_{ej}\right)\left(\sum_{j=1}^3 U_{ej}T^*_{ej}\right)^*\right].\end{aligned}\tag{34}$$

With help of (23) and by assuming (27), $U_0\simeq V_0$ and $(g'_V/g_V)\simeq 1$ we get

$$\begin{aligned}\langle\lambda\rangle&\approx\left(M_{W_1}/M_{W_2}\right)^2\frac{m_D}{m_{\rm LNV}}|\xi|,\\\langle\eta\rangle&\approx-\tan\zeta\,\frac{m_D}{m_{\rm LNV}}|\xi|,\end{aligned}\tag{35}$$

with

$$|\xi| = \left|c_{23}c_{12}^2c_{13}s_{13}^2 - c_{12}^3c_{13}^3 - c_{13}c_{23}c_{12}^2s_{13}^2 - c_{12}c_{13}\left(c_{13}^2s_{12}^2 + s_{13}^2\right)\right| \simeq 0.82 \quad (36)$$

Here, $c_{ij} \equiv \cos(\theta_{ij})$ and $s_{ij} \equiv \sin(\theta_{ij})$. ξ was evaluated by assuming the best fit values for mixing angles θ_{12}, θ_{13}, and θ_{23} entering the PMNS matrix [19]. The experimental upper bound on the mixing angle of left and right vector bosons is $\zeta < 0.013$, and if the CP violating phase in the mixing matrix for right-handed quarks is small one gets $\zeta < 0.0025$. The flavor and CP violating processes of kaons and B mesons make it possible to deduce the lower bound on the mass of the heavy vector boson $M_{W_2} > 2.9$ TeV [11]. In the LRSM there could be additional contributions to $0\nu\beta\beta$ decay due to the double charged Higgs triplet. However, as pointed in Ref. [11], in the considered case of type-I seesaw dominance, these contributions can be neglected.

The coefficients C_I ($I = mm$, $m\lambda$, $m\eta$, $\lambda\lambda$, $\eta\eta$, and $\lambda\eta$) are expressed as combinations of nuclear matrix elements and phase-space factors:

$$\begin{aligned}
C_{mm} &= (1 - \chi_F + \chi_T)^2 G_{01},\\
C_{m\lambda} &= -(1 - \chi_F + \chi_T)[\chi_{2-}G_{03} - \chi_{1+}G_{04}],\\
C_{m\eta} &= (1 - \chi_F + \chi_T)[\chi_{2+}G_{03} - \chi_{1-}G_{04} - \chi_P G_{05} + \chi_R G_{06}],\\
C_{\lambda\lambda} &= \chi_{2-}^2 G_{02} + \tfrac{1}{9}\chi_{1+}^2 G_{011} - \tfrac{2}{9}\chi_{1+}\chi_{2-}G_{010},\\
C_{\eta\eta} &= \chi_{2+}^2 G_{02} + \tfrac{1}{9}\chi_{1-}^2 G_{011} - \tfrac{2}{9}\chi_{1-}\chi_{2+}G_{010} + \chi_P^2 G_{08} - \chi_P\chi_R G_{07} + \chi_R^2 G_{09},\\
C_{\lambda\eta} &= -2\big[\chi_{2-}\chi_{2+}G_{02} - \tfrac{1}{9}(\chi_{1+}\chi_{2+} + \chi_{2-}\chi_{1-})G_{010} + \tfrac{1}{9}\chi_{1+}\chi_{1-}G_{011}\big].
\end{aligned} \quad (37)$$

The explicit form of nuclear matrix elements M_{GT} and their ratios χ_I are presented in Sec. III B. The integrated kinematical factors are defined as

$$\begin{aligned}
G_{0k} &= \frac{G_\beta^4 m_e^2}{64\pi^5 \ln 2 R^2}\int \delta(\varepsilon_1 + \varepsilon_2 + M_f - M_i)\\
&\quad\times [h_{0k}(\varepsilon_1,\varepsilon_2,R)\cos\theta + g_{0k}(\varepsilon_1,\varepsilon_2,R)]\\
&\quad\times p_1 p_2 \varepsilon_1\varepsilon_2 d\varepsilon_1 d\varepsilon_2 d(\cos\theta)\\
&= \int_{-1}^{1}\left(\frac{G_{0k}^\theta}{\ln 2}\cos\theta + \frac{G_{0k}}{2}\right)d(\cos\theta),
\end{aligned} \quad (38)$$

where $k = 1,2,\ldots,11$. p_1 and p_2 are momenta of electrons and θ is the angle between emitted electrons. The functions $h_{0k}(\varepsilon_1,\varepsilon_2,R)$ and $g_{0k}(\varepsilon_1,\varepsilon_2,R)$ are defined in Sec. III A. These definitions are independent of the weak axial-vector coupling constant g_A. The quantities G_{0k} are given in units of inverse years. We note that if the standard wave functions of electron (w.f. A) are assumed, $G_{010} = G_{03}$ and $G_{011} = G_{04}$. If in addition contributions from the induced pseudoscalar term of nucleon current are neglected, the decay rate in Eq. (33) reduces to that given in Ref. [6]. Quantity G_{0k}^θ is relevant for the angular correlation between the two electrons. We note that $G_{03}^\theta = G_{06}^\theta = 0$.

A. Components due to electron wave functions in the phase-space factors

The $s_{1/2}$ and $p_{1/2}$ electron wave functions at the nuclear surface associated with emission of both electrons enter into the phase-space factors through the functions presented below.

For phase-space factors G_{0k}^θ related with the angular distribution of emitted electrons the quantities $h_{0k}(\epsilon_1,\epsilon_2,R)$ are

$$\begin{aligned}
h_{01} &= -4C_{ss}(\varepsilon_1)C_{ss}(\varepsilon_2),\\
h_{02} &= \frac{2\varepsilon_{12}^2}{m_e^2}C_{ss}(\varepsilon_1)C_{ss}(\varepsilon_2),\\
h_{03} &= 0,\\
h_{04} &= -\frac{2}{3m_eR}\left[C_{sp}^f(\varepsilon_1)C_{ss}(\varepsilon_2) + C_{sp}^f(\varepsilon_2)C_{ss}(\varepsilon_1) + C_{sp}^g(\varepsilon_2)C_{ss}(\varepsilon_1) + C_{sp}^g(\varepsilon_1)C_{ss}(\varepsilon_2)\right],\\
h_{05} &= \frac{4}{m_eR}\left[C_{sp}^f(\varepsilon_1)C_{ss}(\varepsilon_2) + C_{sp}^f(\varepsilon_2)C_{ss}(\varepsilon_1) + C_{sp}^g(\varepsilon_2)C_{ss}(\varepsilon_1) + C_{sp}^g(\varepsilon_1)C_{ss}(\varepsilon_2)\right],\\
h_{06} &= 0,\\
h_{07} &= \frac{-16}{(m_eR)^2}\left[C_{sp}^f(\varepsilon_1)C_{ss}(\varepsilon_2) + C_{sp}^f(\varepsilon_2)C_{ss}(\varepsilon_1) - C_{sp}^g(\varepsilon_2)C_{ss}(\varepsilon_1) - C_{sp}^g(\varepsilon_1)C_{ss}(\varepsilon_2)\right],\\
h_{08} &= \frac{-8}{(m_eR)^2}\left[C_{sp}^f(\varepsilon_1)C_{sp}^g(\varepsilon_2) + C_{sp}^f(\varepsilon_2)C_{sp}^g(\varepsilon_1) + C_{ss}(\varepsilon_1)C_{pp}(\varepsilon_2) + C_{ss}(\varepsilon_2)C_{pp}(\varepsilon_1)\right],\\
h_{09} &= \frac{32}{(m_eR)^2}C_{ss}(\varepsilon_1)C_{ss}(\varepsilon_2),\\
h_{010} &= -\frac{9}{2}\tilde{h}_{010} - h_{02},\\
h_{011} &= 9\tilde{h}_{011} + \frac{1}{9}h_{02} + \tilde{h}_{010},
\end{aligned} \quad (39)$$

with

$$\tilde{h}_{010} = \frac{2\varepsilon_{12}}{3m_e^2 R}\left[C_{sp}^f(\varepsilon_1)C_{ss}(\varepsilon_2) - C_{sp}^f(\varepsilon_2)C_{ss}(\varepsilon_1) + C_{sp}^g(\varepsilon_2)C_{ss}(\varepsilon_1) - C_{sp}^g(\varepsilon_1)C_{ss}(\varepsilon_2)\right],$$
$$\tilde{h}_{011} = \frac{-2}{(3m_e R)^2}\left[C_{sp}^f(\varepsilon_1)C_{sp}^f(\varepsilon_2) + C_{sp}^g(\varepsilon_2)C_{sp}^g(\varepsilon_1) + C_{ss}(\varepsilon_1)C_{pp}(\varepsilon_2) + C_{ss}(\varepsilon_2)C_{pp}(\varepsilon_1)\right]. \quad (40)$$

In addition, the components $g_{0k}(\epsilon_1,\epsilon_2,R)$ of the phase-space factors (38) are

$$g_{01} = g_{11} = C_{ss}^+(\varepsilon_1)C_{ss}^+(\varepsilon_2),$$
$$g_{02} = \frac{\varepsilon_{12}^2}{2m_e^2}[C_{ss}^+(\varepsilon_1)C_{ss}^+(\varepsilon_2) - C_{ss}^-(\varepsilon_1)C_{ss}^-(\varepsilon_2)],$$
$$g_{03} = \frac{\varepsilon_{12}}{m_e}[C_{ss}^+(\varepsilon_1)C_{ss}^-(\varepsilon_2) - C_{ss}^+(\varepsilon_2)C_{ss}^-(\varepsilon_1)],$$
$$g_{04} = \frac{1}{3m_e R}[-C_{ss}^-(\varepsilon_1)C_{sp}^-(\varepsilon_2) - C_{ss}^-(\varepsilon_2)C_{sp}^-(\varepsilon_1) + C_{ss}^+(\varepsilon_1)C_{sp}^+(\varepsilon_2) + C_{ss}^+(\varepsilon_2)C_{sp}^+(\varepsilon_1)] - g_{03}/9,$$
$$g_{05} = \frac{-2}{m_e R}[C_{ss}^-(\varepsilon_1)C_{sp}^-(\varepsilon_2) + C_{ss}^-(\varepsilon_2)C_{sp}^-(\varepsilon_1) + C_{ss}^+(\varepsilon_1)C_{sp}^+(\varepsilon_2) + C_{ss}^+(\varepsilon_2)C_{sp}^+(\varepsilon_1)],$$
$$g_{06} = \frac{4}{m_e R}[C_{ss}^+(\varepsilon_1)C_{ss}^-(\varepsilon_2) + C_{ss}^+(\varepsilon_2)C_{ss}^-(\varepsilon_1)], \quad (41)$$
$$g_{07} = \frac{-8}{(m_e R)^2}[C_{ss}^+(\varepsilon_1)C_{sp}^-(\varepsilon_2) + C_{ss}^+(\varepsilon_2)C_{sp}^-(\varepsilon_1) + C_{ss}^-(\varepsilon_1)C_{sp}^+(\varepsilon_2) + C_{ss}^-(\varepsilon_2)C_{sp}^+(\varepsilon_1)],$$
$$g_{08} = \frac{2}{(m_e R)^2}[-C_{pp}^-(\varepsilon_1)C_{ss}^-(\varepsilon_2) - C_{pp}^-(\varepsilon_2)C_{ss}^-(\varepsilon_1) + C_{pp}^+(\varepsilon_1)C_{ss}^+(\varepsilon_2) + C_{pp}^+(\varepsilon_2)C_{ss}^+(\varepsilon_1) + 2C_{sp}^-(\varepsilon_1)C_{sp}^-(\varepsilon_2) + 2C_{sp}^+(\varepsilon_1)C_{sp}^+(\varepsilon_2)],$$
$$g_{09} = \frac{8}{(m_e R)^2}[C_{ss}^+(\varepsilon_1)C_{ss}^+(\varepsilon_2) + C_{ss}^-(\varepsilon_1)C_{ss}^-(\varepsilon_2)],$$
$$g_{010} = -\frac{9}{2}\tilde{g}_{010} - g_{02},$$
$$g_{011} = 9\tilde{g}_{011} + \frac{1}{9}g_{02} + \tilde{g}_{010},$$

with

$$\tilde{g}_{010} = \frac{\varepsilon_{12}}{3m_e^2 R}[-C_{ss}^+(\varepsilon_1)C_{sp}^-(\varepsilon_2) + C_{ss}^+(\varepsilon_2)C_{sp}^-(\varepsilon_1) + C_{ss}^-(\varepsilon_1)C_{sp}^+(\varepsilon_2) - C_{ss}^-(\varepsilon_2)C_{sp}^+(\varepsilon_1)],$$
$$\tilde{g}_{011} = \frac{1}{18m_e^2 R^2}[C_{pp}^-(\varepsilon_1)C_{ss}^-(\varepsilon_2) + C_{pp}^-(\varepsilon_2)C_{ss}^-(\varepsilon_1) + C_{pp}^+(\varepsilon_1)C_{ss}^+(\varepsilon_2) + C_{pp}^+(\varepsilon_2)C_{ss}^+(\varepsilon_1) - 2C_{sp}^-(\varepsilon_1)C_{sp}^-(\varepsilon_2) + 2C_{sp}^+(\varepsilon_1)C_{sp}^+(\varepsilon_2)]. \quad (42)$$

Here, C are combinations of radial components of $s_{1/2}$ and $p_{1/2}$ wave functions,

$$C_{ss}(\varepsilon) = g_{-1}(\varepsilon)f_{+1}(\varepsilon), \quad C_{pp}(\varepsilon_1) = g_1(\varepsilon)f_{-1}(\varepsilon), \quad C_{sp}^f(\varepsilon) = f_{-1}(\varepsilon)f_{+1}(\varepsilon), \quad C_{sp}^g(\varepsilon) = g_{-1}(\varepsilon)g_{+1}(\varepsilon),$$
$$C_{ss}^\pm(\varepsilon) = g_{-1}^2(\varepsilon) \pm f_{+1}^2(\varepsilon), \quad C_{pp}^\pm(\varepsilon) = g_{+1}^2(\varepsilon) \pm f_{-1}^2(\varepsilon), \quad C_{sp}^\pm(\varepsilon) = g_{-1}(\varepsilon)f_{-1}(\varepsilon) \pm g_{+1}(\varepsilon)f_{+1}(\varepsilon). \quad (43)$$

B. Nuclear matrix elements entering the decay rate

The expression for the $0\nu\beta\beta$-decay half-life in Eq. (33) contains matrix element ratios χ_I and their linear combinations $\chi_{1\pm}$ and $\chi_{2\pm}$. The quantities χ_I are defined as

$$\chi_I = M_I/M_{GT}, \quad (44)$$

where $I = F, T, \omega F, \omega GT, \omega T, qF, qGT, qT, R$, and P and M_{GT} is the dominant Gamow-Teller matrix element associated with the mechanism due to the left-handed currents. The combinations $\chi_{1\pm}$ and $\chi_{2\pm}$ are given by

$$\chi_{1\pm} = \chi_{qGT} - 6\chi_{qT} \pm 3\chi_{qF}, \quad \chi_{2\pm} = \chi_{GT\omega} + \chi_{T\omega} \pm \chi_{F\omega} - \tfrac{1}{9}\chi_{1\mp}. \quad (45)$$

The nuclear matrix elements M_I depend on the exchange potentials $h_I(r)$ through

$$\begin{aligned}
M_{F,GT,T} &= \sum_{rs}\langle A_f\|h_{F,GT,T}(r_-)\mathcal{O}_{F,GT,T}\|A_i\rangle,\\
M_{\omega F,\omega GT,\omega T} &= \sum_{rs}\langle A_f\|h_{\omega F,\omega GT,\omega T}(r_-)\mathcal{O}_{F,GT,T}\|A_i\rangle,\\
M_P &= \sum_{rs} i\langle A_f\|h_P(r_-)\tau_r^+\tau_s^+\frac{(\mathbf{r}_-\times\mathbf{r}_+)}{R^2}\cdot\vec{\sigma}_r\|A_i\rangle,\\
M_{qF,qGT,qT} &= \sum_{rs}\langle A_f\|h_{qF,qGT,qT}(r_-)\mathcal{O}_{F,GT,T}\|A_i\rangle,\\
M_R &= \sum_{rs}\langle A_f\|[h_{RG}(r_-)\mathcal{O}_{GT}+h_{RT}(r_-)\mathcal{O}_T]\|A_i\rangle,
\end{aligned}$$

where $\mathcal{O}_{F,GT,T}$ are the familiar operators $1,\vec{\sigma}_1\cdot\vec{\sigma}_2$ and $3(\vec{\sigma}_1\cdot\hat{r}_{12})(\vec{\sigma}_2\cdot\hat{r}_{12})$.

The two-nucleon exchange potentials $h_I(r)$ with F, GT, T, qF, qGT, qT, RG, RT, and P can be written as

$$h_I(r) = \frac{2R}{\pi}\int f_I(q,r)\frac{q\,dq}{q+\bar{E}_n-(E_i+E_f)/2}, \tag{46}$$

where

$$\begin{aligned}
f_{GT} &= \frac{j_0(q,r)}{g_A^2}\left(g_A^2(q^2)-\frac{g_A(q^2)g_P(q^2)}{m_N}\frac{q^2}{3}+\frac{g_P^2(q^2)}{4m_N^2}\frac{q^4}{3}\right),\\
f_F &= \frac{g_V^2(q^2)}{g_A^2}j_0(qr),\\
f_T &= \frac{j_2(q,r)}{g_A^2}\left(\frac{g_A(q^2)g_P(q^2)}{m_N}\frac{q^2}{3}-\frac{g_P^2(q^2)}{4m_N^2}\frac{q^4}{3}\right),\\
f_{qF} &= r\frac{g_V^2(q^2)}{g_A^2}j_1(qr)q,\\
f_{qGT} &= \left(\frac{g_A^2(q^2)}{g_A^2}q+3\frac{g_P^2(q^2)}{g_A^2}\frac{q^5}{4m_N^2}+\frac{g_A(q^2)g_P(q^2)}{g_A^2}\frac{q^3}{m_N}\right)rj_1(qr),\\
f_{qT} &= \frac{r}{3}\left[\left(\frac{g_A^2(q^2)}{g_A^2}q-\frac{g_P(q^2)g_A(q^2)}{2g_A^2}\frac{q^3}{m_N}\right)j_1(qr)-9\frac{g_P^2(q^2)}{2g_A^2}\frac{q^5}{20m_N^2}[2j_1(qr)/3-j_3(qr)]\right],\\
f_{RG} &= \frac{-R}{3m_N}\left(1+\frac{g_M(q^2)}{g_V(q^2)}\right)\frac{g_A(q^2)g_V(q^2)}{g_A^2}j_0(qr)q^2,\\
f_{RT} &= \frac{-R}{6m_N}\left(1+\frac{g_M(q^2)}{g_V(q^2)}\right)\frac{g_A(q^2)g_V(q^2)}{g_A^2}j_2(qr)q^2,\\
f_P &= \frac{R^2}{r}\frac{g_V(q^2)g_A(q^2)}{g_A^2}j_1(qr)q.
\end{aligned} \tag{47}$$

The two-nucleon exchange potentials $h_I(r)$ with $I=\omega F$, ωGT, and ωT take the form

$$h_I(r) = \frac{4R}{\pi}\int f_I(q,r)\frac{q^2dq}{[q+\bar{E}_n-(E_i+E_f)/2]^2}, \tag{48}$$

where

$$f_{\omega F}=f_F,\quad f_{\omega GT}=f_{GT},\quad f_{\omega T}=f_T. \tag{49}$$

Here, $\mathbf{r}_+=(\mathbf{r}_r+\mathbf{r}_s)/2$, $\mathbf{r}_-=(\mathbf{r}_r-\mathbf{r}_s)$. $\mathbf{r}_{r,s}$ is the coordinate of the decaying nucleon and $j_i(qr)$ $(i=1,2,3)$ are the spherical Bessel functions. It is assumed that $\mathbf{p}_r+\mathbf{p}'_r\simeq 0$, $E_r-E'_r\simeq 0$, and $\mathbf{p}_r-\mathbf{p}'_r\simeq\mathbf{q}$, where $\mathbf{q}$ is the momentum exchange. The form factors $g_V(q^2)$, $g_A(q^2)$, $g_M(q^2)$, and $g_V(q^2)$ are defined in Ref. [20] and $g_A=1.269$.

If right-handed currents are switched off, all terms in Eq. (33) except that proportional to C_1 vanish. The connection with the standard $0\nu\beta\beta$-decay formula (33) is then $G_{01}\equiv G^{0\nu}$ and $M_{GT}(1-\chi_F+\chi_T)\equiv M^{0\nu}$.

TABLE I. Phase-space factors G_{0k} (k=1, ..., 11) in units yr^{-1} for the $0\nu\beta\beta$ decay of ^{76}Ge, ^{130}Te, and ^{150}Nd. Calculation was performed by assuming different approximations for the radial wave functions $g_{\pm1}$ and $f_{\pm1}$ of an electron: (A) The standard approximation of Doi *et al.* [6]. (B) An analytical solution of Dirac equations for a pointlike nucleus is assumed. (C) An exact solution of Dirac equations for a uniform charge distribution in nucleus is considered. (D) The same as the preceding case but the electron screening is taken into account [3].

w.f.	^{76}Ge				^{130}Te				^{150}Nd			
	A	B	C	D	A	B	C	D	A	B	C	D
$10^{14}G_{01}$	0.261	0.244	0.240	0.237	1.807	1.535	1.453	1.425	8.827	6.986	6.432	6.316
$10^{14}G_{02}$	0.428	0.404	0.397	0.391	4.683	4.064	3.851	3.761	40.190	32.401	29.869	29.187
$10^{15}G_{03}$	1.478	1.340	1.316	1.305	12.237	9.566	9.065	8.967	70.032	49.465	45.593	45.130
$10^{15}G_{04}$	0.501	0.489	0.477	0.470	3.625	3.315	3.086	3.021	18.343	16.000	14.348	14.066
$10^{13}G_{05}$	0.791	0.727	0.572	0.566	6.390	5.185	3.842	3.790	28.537	21.183	15.061	14.873
$10^{12}G_{06}$	0.605	0.547	0.536	0.531	3.091	2.398	2.258	2.227	11.922	8.323	7.591	7.497
$10^{10}G_{07}$	0.365	0.345	0.274	0.270	2.713	2.383	1.788	1.755	13.625	11.362	8.233	8.085
$10^{11}G_{08}$	0.245	0.236	0.151	0.149	2.877	2.653	1.579	1.549	16.833	14.996	8.564	8.405
$10^{10}G_{09}$	1.360	1.263	1.238	1.223	6.398	5.354	5.063	4.972	27.582	21.530	19.799	19.454
$10^{15}G_{010}$	1.478	1.531	1.423	1.410	12.237	14.602	11.616	11.455	70.032	105.415	72.249	71.154
$10^{15}G_{011}$	0.501	0.500	0.484	0.476	3.625	3.564	3.220	3.148	18.343	18.334	15.376	15.055

IV. PHASE-SPACE FACTORS WITH IMPROVED ACCURACY

In Sec. II different ways of treating the radial wave functions $g_{\pm1}(\varepsilon,r)$ and $f_{\pm1}(\varepsilon,r)$ associated with emitted electrons in the $s_{1/2}$ and $p_{1/2}$ wave states were presented. The derivation of the $0\nu\beta\beta$-decay rate was accomplished by considering electron wave functions for the pointlike nucleus (wave function B) or an extended one (wave functions A, C, and D); that allowed us to separate phase-space factors and nuclear matrix elements. The accuracy of the calculation of phase-space factors will be discussed next and the improved phase-space factors associated with mechanisms due to right-handed currents obtained using screened exact finite-size Coulomb wave functions of emitted electrons (wave functions D) will be presented.

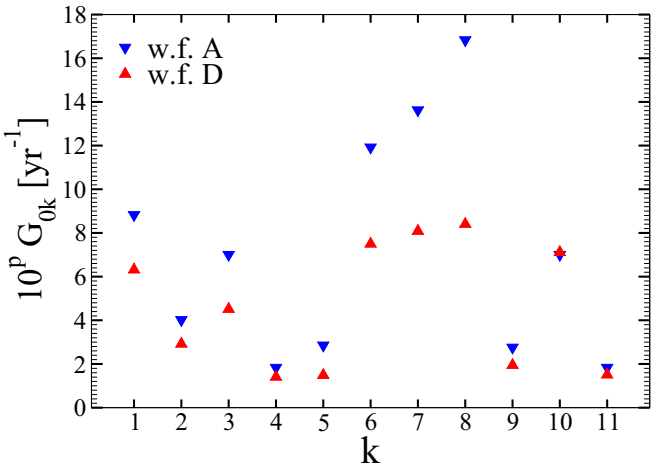

FIG. 2. (Color online) The phase factors G_{0k} ($k = 1, \ldots, 11$) in units of yr^{-1} for the $0\nu\beta\beta$ decay of ^{150}Nd. Results are presented for approximate electron wave functions (type A [6]) and exact Dirac wave functions with finite nuclear size and electron screening (type D [3]). The exponents p for $k = 1, \ldots, 11$ are 14,14,15,15,13,12,10,11,10,15,15, respectively.

A numerical computation of all eleven phase-space factors entering the $0\nu\beta\beta$-decay rate was performed by using the previously described four types of wave functions (A, B, C, and D) for a sample of three isotopes (^{76}Ge, ^{130}Te, and ^{150}Nd). Results are presented in Table I. We see that by using the standard treatment of electron wave functions, corresponding to leading finite-size Coulomb corrections (wave functions A), a significant difference with the results of the other three approaches appears, especially for nuclei with large nuclear charge Z. Surprisingly, results obtained with wave functions B, corresponding to an analytical solution of Dirac equations for a pointlike nucleus, better agree with results corresponding to wave functions C and D (exact solution of Dirac equations for a uniform nuclear charge distribution with the radius R) than those obtained by the standard treatment of wave functions (wave functions A). This indicates that the exact treatment of the Coulomb field plays a more important role than the position of the decaying nucleon in the nucleus. From the Table I it is

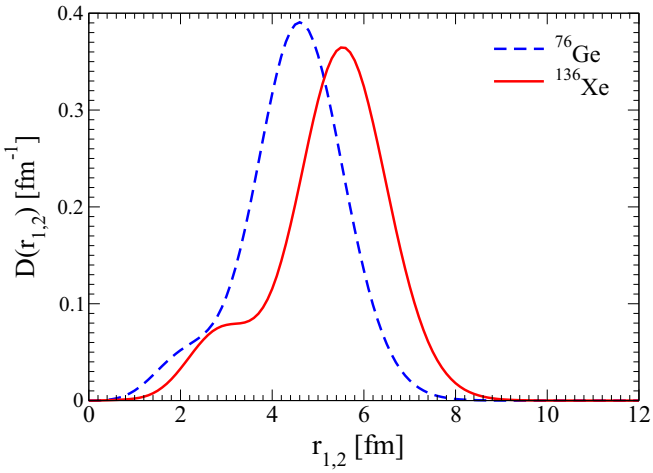

FIG. 3. (Color online) The normalized r_1 (r_2) dependence of $M^{0\nu}$ for ^{76}Ge and ^{136}Xe. r_1 and r_2 are absolute values of a position vector of the β-decaying nucleon in a nucleus.

TABLE II. The phase-space factor G_{01} in units yr^{-1} for the $0\nu\beta\beta$ decay of ^{76}Ge, ^{130}Te, and ^{136}Xe. Results are presented for exact Dirac wave functions with finite nuclear size and electron screening at nuclear radius R (exact, approximation scheme D) and those averaged over the distribution deduced from the analysis of the dominant nuclear matrix element [exact and averaged; see Eqs. (50)].

	$10^{14}G_{01}$		
	^{76}Ge	^{130}Te	^{136}Xe
Exact	0.23681	1.42547	1.46187
Exact and averaged	0.23987	1.47396	1.52851

apparent that the effect of the screening of atomic electrons on the wave functions of emitted electrons does not play an important role.

The phase-factors differ among themselves significantly in magnitude. This fact is manifested in Fig. 2. One can see that phase-factors obtained with standard wave functions (w.f. A) are always larger than those with phase factors calculated with the more advanced wave functions. Exact treatment reduces the value of all studied phase-space factors.

The phase-space factors [see Eq. (38)] contain products of $g_{\pm1}(\varepsilon)$ and $f_{\pm1}(\varepsilon)$, which were evaluated at $r = R$ from radial wave functions $g_{\pm1}(\varepsilon,r)$ and $f_{\pm1}(\varepsilon,r)$ [see Eq. (32)]. Thus, it is assumed that the β decay of both nucleons happens at the nuclear surface. This procedure can be generalized with the help of the normalized-to-unity distribution function $D(r_1)$ as follows:

$$g_{\pm1}(\varepsilon,R) = \int_0^\infty g_{\pm1}(\varepsilon,r_1)D(r_1)dr_1,$$
$$f_{\pm1}(\varepsilon,R) = \int_0^\infty f_{\pm1}(\varepsilon,r_1)D(r_1)dr_1, \quad (50)$$

where in this particular case $D(r_1) = \delta(r_1 - R)$.

In Fig. 3 the distribution function $D(r_1)$ [or equivalently $D(r_2)$] is shown corresponding to the nuclear matrix element $M^{0\nu}$ (associated with the $m_{\beta\beta}$ mechanism) of the $0\nu\beta\beta$ decay of ^{76}Ge and ^{136}Xe and calculated within the quasiparticle random phase approximation with restoration of isospin symmetry [21]. We see that β decay of both nucleons happens mostly in the vicinity of the nuclear surface. In Table II the phase-space factor G_{01} calculated with the help of $D(r_1) = \delta(r_1 - R)$ and $D(r_1)$ deduced from calculated nuclear matrix elements of ^{76}Ge, ^{130}Te, and ^{136}Xe are compared. We see that the corresponding effect is very small for ^{76}Ge and is only about 4–5% in the cases of ^{130}Te and ^{136}Xe.

The improved phase-space factors G_{0j} ($j = 1,\ldots,11$) in units yr^{-1} associated with left- and right-handed mechanisms of the $0\nu\beta\beta$ decay for nuclei of experimental interest are presented in Table III. They were obtained using screened exact finite-size Coulomb wave functions for $s_{1/2}$ and $p_{1/2}$ electron states (wave functions D). In Table IV the phase-space factors G^{θ}_{0j} associated with angular distribution of emitted electrons are presented.

V. CONSTRAINTS ON THE EFFECTIVE TOTAL LEPTON-NUMBER-VIOLATING PARAMETERS

Experimental $0\nu\beta\beta$-decay half-life limits may be used, in combination with the formula (33), to constrain the effective Majorana neutrino mass $m_{\beta\beta}$ and the effective coupling constants $\langle\lambda\rangle$ and $\langle\eta\rangle$ of the right-handed currents. This can be done provided the values of phase-space factors and nuclear matrix elements are available. We use the quasiparticle random phase approximation (QRPA) [22] and interacting shell model (ISM) [23] matrix elements for such analysis. Their values are presented in Table V. In the case of ISM the magnitudes of matrix elements M_{GT} calculated in Ref. [24] are assumed. We note that these matrix elements were evaluated when the contribution from the induced pseudoscalar term of hadron current was not taken into account. In the analysis below the case of CP conservation ($\psi_1 = \psi_2 = 0$) is assumed.

Different contributions to the $0\nu\beta\beta$-decay rate (33) are associated with different products of effective lepton number violating parameters $m_{\beta\beta}$, $\langle\lambda\rangle$, and $\langle\eta\rangle$, whose values are

TABLE III. Phase-space factors G_{0j} ($j = 1,\ldots,11$) in units yr^{-1} obtained using screened exact finite-size Coulomb wave functions for $s_{1/2}$ and $p_{1/2}$ electron states (wave functions D). The Q values were taken from experiment when available, or from tables of recommended value [3]. G_{01} is associated with the mechanism generated just by $m_{\beta\beta}$. In the case of dominance of the $\langle\lambda\rangle$ ($\langle\eta\rangle$) mechanism the decay rate includes phase factors G_{02}, G_{010}, and G_{011} (G_{02}, G_{07}, G_{08}, G_{09}, G_{010}, and G_{011}). The remaining phase factors are due to interference of these mechanisms [see Eq. (38)].

	^{48}Ca	^{76}Ge	^{82}Se	^{96}Zr	^{100}Mo	^{110}Pd	^{116}Cd	^{124}Sn	^{130}Te	^{136}Xe	^{150}Nd
$Q_{\beta\beta}$ (MeV)	4.27226	2.03904	2.99512	3.35037	3.03440	2.01785	2.8135	2.28697	2.52697	2.45783	3.37138
$10^{14}G_{01}$	2.483	0.237	1.018	2.062	1.595	0.483	1.673	0.906	1.425	1.462	6.316
$10^{14}G_{02}$	16.229	0.391	3.529	8.959	5.787	0.814	5.349	1.967	3.761	3.679	29.187
$10^{15}G_{03}$	18.907	1.305	6.913	14.777	10.974	2.672	11.128	5.403	8.967	9.047	45.130
$10^{15}G_{04}$	5.327	0.470	2.141	4.429	3.400	0.978	3.569	1.886	3.021	3.099	14.066
$10^{13}G_{05}$	3.007	0.566	2.004	4.120	3.484	1.400	4.060	2.517	3.790	4.015	14.873
$10^{12}G_{06}$	3.984	0.531	1.733	3.043	2.478	0.934	2.563	1.543	2.227	2.275	7.497
$10^{10}G_{07}$	2.682	0.270	1.163	2.459	1.927	0.599	2.062	1.113	1.755	1.812	8.085
$10^{11}G_{08}$	1.109	0.149	0.708	1.755	1.420	0.462	1.703	0.939	1.549	1.657	8.405
$10^{10}G_{09}$	16.246	1.223	4.779	8.619	6.540	1.939	6.243	3.301	4.972	4.956	19.454
$10^{14}G_{010}$	2.116	0.141	0.801	1.855	1.359	0.309	1.418	0.660	1.146	1.165	7.115
$10^{15}G_{011}$	5.376	0.476	2.183	4.557	3.502	1.010	3.704	1.955	3.148	3.238	15.055

TABLE IV. Phase-space factors G^{θ}_{0j} associated with angular distribution of emitted electrons [see Eq. (38)] in units yr^{-1} obtained using screened exact finite-size Coulomb wave functions for $s_{1/2}$ and $p_{1/2}$ electron states (wave functions D). The Q values of Table III are assumed.

	^{48}Ca	^{76}Ge	^{82}Se	^{96}Zr	^{100}Mo	^{110}Pd	^{116}Cd	^{124}Sn	^{130}Te	^{136}Xe	^{150}Nd
$-10^{15}G^{\theta}_{01}$	8.010	0.679	3.141	6.484	4.951	1.397	5.153	2.699	4.328	4.426	20.101
$10^{14}G^{\theta}_{02}$	5.144	0.113	1.075	2.769	1.770	0.239	1.629	0.587	1.137	1.111	9.138
$-10^{15}G^{\theta}_{04}$	1.786	0.152	0.703	1.456	1.112	0.314	1.161	0.608	0.977	1.000	4.566
$10^{15}G^{\theta}_{05}$	10.714	0.910	4.219	8.734	6.674	1.884	6.965	3.650	5.862	6.002	27.397
$10^{11}G^{\theta}_{07}$	8.458	0.711	3.422	7.431	5.706	1.589	6.026	3.089	5.016	5.155	24.824
$10^{12}G^{\theta}_{08}$	3.553	0.402	2.121	5.383	4.271	1.251	5.054	2.651	4.498	4.787	26.100
$10^{10}G^{\theta}_{09}$	5.024	0.313	1.379	2.562	1.904	0.504	1.795	0.899	1.397	1.387	5.899
$10^{15}G^{\theta}_{010}$	0.695	0.028	0.317	1.118	0.764	0.114	0.884	0.334	0.706	0.741	7.816
$-10^{15}G^{\theta}_{011}$	1.790	0.152	0.707	1.466	1.120	0.317	1.172	0.615	0.988	1.012	4.594

unknown. The importance of these contributions depends also on the value coefficients C_I ($I = mm$, $m\lambda$, $m\eta$, $\lambda\lambda$, $\eta\eta$, and $\lambda\eta$, which can be calculated. The quantity is a superposition of contributions C^{0k}_I associated with phase-spase factors G_{0k} ($k = 1, \ldots, 11$). In Fig. 4 we show ratios C^{0k}_I/C_I for the $0\nu\beta\beta$ decay ^{76}Ge and ^{136}Xe and both sets of nuclear matrix elements. We note that coefficients C_{mm}, $C_{\lambda\lambda}$, $C_{\eta\eta}$, and $C_{m\eta}$ are dominated by a single contribution associated with a different phase factor. In the case of $C_{m\lambda}$ and $C_{\lambda\eta}$ there is a competition of mostly two contributions.

Using these nuclear matrix elements (Table V) and the phase-space factors calculated here (see Table III) we can deduce from the experimental data $T^{0\nu}_{1/2} \geqslant 3.010^{25}$ yr for ^{76}Ge decay [25] and $T^{0\nu}_{1/2} \geqslant 3.410^{25}$ yr for ^{136}Xe decay [26] (we use here the combined limit from the EXO and KamLAND-Zen experiments) the constraints on the effective right-handed current couplings $\langle\lambda\rangle$, $\langle\eta\rangle$ and the effective Majorana neutrino mass $m_{\beta\beta}$ listed in Table VI. The constraints in Table VI are of a similar magnitude as those in Table I of Ref. [11]. However, they are based now on the exact treatment of the phase-space factors as well as on the more complete account of nuclear matrix elements. Figure 5 shows the allowed regions for $m_{\beta\beta}$ and $\langle\lambda\rangle$ ($\langle\eta\rangle$) for $\langle\eta\rangle = 0$ ($\langle\lambda\rangle = 0$). Results are presented for the two sets of nuclear matrix elements (ISM [23,24] and QRPA [22]) and the standard (w.f. A) and improved (w.f. D) description of electron wave functions.

TABLE V. Nuclear matrix elements and their ratios. The quasiparticle random phase approximation (QRPA) and interacting shell model (ISM) matrix elements are from [22,23], respectively. In the case of ISM matrix elements M_{GT} calculated in Ref. [24] is used.

	^{76}Ge		^{136}Xe	
	ISM	QRPA	ISM	QRPA
M_{GT}	2.350	3.014	1.770	1.120
χ_F	−0.106	−0.389	−0.151	−0.412
χ_{1+}	0.686	0.811	0.782	1.969
χ_{1-}	1.340	2.917	1.784	4.052
χ_{2+}	0.633	0.302	0.556	0.229
χ_{2-}	0.912	1.216	0.965	1.195
χ_R	0.684	1.192	0.955	1.958
χ_P	−0.544	−0.176	0.256	−0.321

Note that limits on lepton number violating parameters are softened a little when other lepton number violating parameters have nonvanishing values at the same time in comparison with the case when only a single parameter is nonzero. By assuming $\zeta = 0.013$ and 0.0025 mentioned earlier and the current limit $\langle\eta\rangle \leqslant 2.9810^{-9}$ (^{136}Xe, ISM, w.f. D) we end up with $m_D/m_{\rm LNV} = 2.810^{-7}$ and 1.510^{-6}, respectively. For $M_{W_2} = 2.9$ TeV and $\langle\lambda\rangle \leqslant 3.3410^{-7}$ (^{136}Xe, ISM, w.f. D) we get $m_D/m_{\rm LNV} = 5.010^{-6}$. Thus, from the more stringent limits on $\langle\eta\rangle$ we obtain $m_{\rm LNV}/{\rm TeV} = 0.3$–$2\ m_D/{\rm MeV}$, in agreement with the assumption that the basic scale of LRSM is O(TeV). It is therefore obvious that already the present limits of $0\nu\beta\beta$-decay half-lives can be used to constrain meaningfully the allowed parameter space of LRSM, and that the mechanism associated with right-handed currents can compete with the one based on $m_{\beta\beta}$ that is so often used.

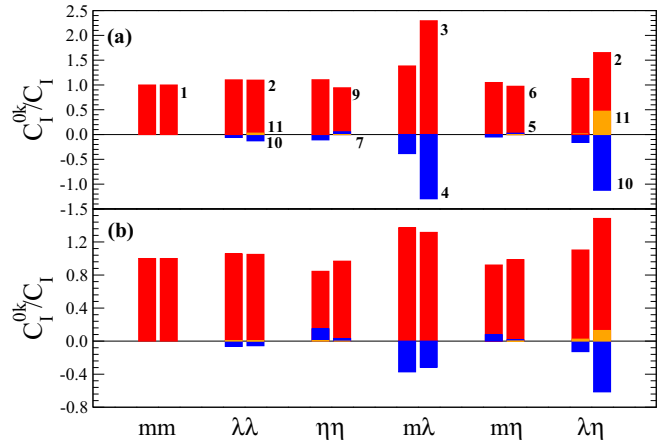

FIG. 4. (Color online) The decomposition of coefficients C_I [$I = mm$, $m\lambda$, $m\eta$, $\lambda\lambda$, $\eta\eta$, and $\lambda\eta$; see Eqs. (33) and (37)] on partial contributions C^{0k}_I associated with phase-space factors G_{0k} ($k = 1, \ldots, 11$). The symbols standing for index I are shown on the x axis. The partial contributions are identified by index k, whose value is shown by the corresponding bar. The contributions from largest to the third largest are displayed in red, blue, and orange colors, respectively. Ratios C^{0k}_I/C_I calculated with the ISM and QRPA matrix elements are presented with left and right bars for each value of index I, respectively. Results for ^{76}Ge and ^{136}Xe are presented in the lower (b) and upper (a) panels, respectively.

TABLE VI. Upper bounds on the effective neutrino mass $m_{\beta\beta}$ and parameters $\langle\eta\rangle$ and $\langle\lambda\rangle$ associated with right-handed currents mechanisms imposed by the constraints on the $0\nu\beta\beta$ decay of ^{76}Ge ($T^{0\nu}_{1/2} \geqslant 3.010^{25}$ yr [25]) and ^{136}Xe ($T^{0\nu}_{1/2} \geqslant 3.410^{25}$ yr [26]). Nuclear matrix elements of the interacting shell model (ISM) [23] (M_{GT} is from [24]) and quasiparticle random phase approximations (QRPA) [22] are used in the analysis. CP conservation is assumed ($\psi_1 = \psi_2 = 0$). The standard electron wave functions (w.f. A) [6] and screened exact finite-size Coulomb wave functions (w.f. D) are considered.

w.f.	^{76}Ge		^{136}Xe	
	A	D	A	D
		QRPA		
$\lvert m_{\beta\beta}\rvert$ (eV)	0.321	0.333	0.285	0.315
$\lvert m_{\beta\beta}\rvert$ (eV) for $\langle\eta\rangle = \langle\lambda\rangle = 0$	0.271	0.284	0.251	0.285
$10^9\langle\eta\rangle$	3.093	3.239	2.077	2.337
$10^9\langle\eta\rangle$ for $\lvert m_{\beta\beta}\rvert = \langle\lambda\rangle = 0$	2.652	2.807	1.840	2.118
$10^7\langle\lambda\rangle$	4.943	5.163	3.822	4.370
$10^7\langle\lambda\rangle$ for $\lvert m_{\beta\beta}\rvert = \langle\eta\rangle = 0$	4.841	5.068	3.792	4.349
		ISM		
$\lvert m_{\beta\beta}\rvert$ (eV)	0.515	0.535	0.222	0.245
$\lvert m_{\beta\beta}\rvert$ (eV) for $\langle\eta\rangle = \langle\lambda\rangle = 0$	0.436	0.458	0.194	0.220
$10^9\langle\eta\rangle$	6.370	6.760	2.975	3.291
$10^9\langle\eta\rangle$ for $\lvert m_{\beta\beta}\rvert = \langle\lambda\rangle = 0$	5.464	5.863	2.628	2.976
$10^7\langle\lambda\rangle$	8.462	8.841	3.000	3.378
$10^7\langle\lambda\rangle$ for $\lvert m_{\beta\beta}\rvert = \langle\eta\rangle = 0$	8.304	8.694	2.949	3.336

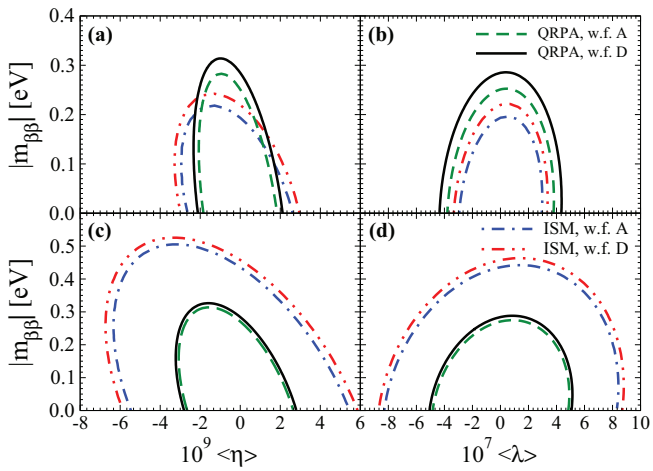

FIG. 5. (Color online) Limits on the effective neutrino mass $m_{\beta\beta}$ and right-handed parameters η (left panels, $\langle\lambda\rangle = 0$) and λ (right panels, $\langle\eta\rangle = 0$) implied by the constraints on the $0\nu\beta\beta$ decay of ^{76}Ge (lower panels, $T^{0\nu}_{1/2} \geqslant 3.010^{25}$ yr [25]) and ^{136}Xe (upper panels, $T^{0\nu}_{1/2} \geqslant 3.410^{25}$ yr [26]). To derive the bounds, the values of nuclear matrix elements calculated within the ISM [23] and the QRPA [22] are used. Results are presented for approximate electron wave functions (type A) and exact Dirac wave functions with finite nuclear size and electron screening (type D). Ellipses show the boundaries of the allowed domains.

VI. DIFFERENTIAL DECAY RATES FOR LIMITING CASES

It is of interest to consider the angular correlations of the emitted electrons and the single-electron energy spectrum for the three limiting cases of lepton number violating mechanism, since with sufficient experimental accuracy one could distinguish between decays due to coupling to the left-handed and right-handed hadronic currents. It is assumed that some future $0\nu\beta\beta$-decay experiments, e.g., the SuperNEMO [27] or NEXT [28], will have a unique potential to measure the electron tracks and thus to observe the decay electron angular correlations and individual electron energy spectra.

The differential rate for the $0^+ \to 0^+$ $0\nu\beta\beta$ decay with the energy of one of the emitted electrons $\tilde{\varepsilon}_1$ ($\tilde{\varepsilon}_1$ is the kinetic energy fraction with respect to $Q_{\beta\beta}$ of one electron, i.e., $\varepsilon_1 = \tilde{\varepsilon}_1 Q_{\beta\beta} + m_e$ and $\varepsilon_2 = Q_{\beta\beta} + 2m_e - \varepsilon_1$) and the angular distribution with the angle θ between the two electrons for three limiting cases can be written as follows:

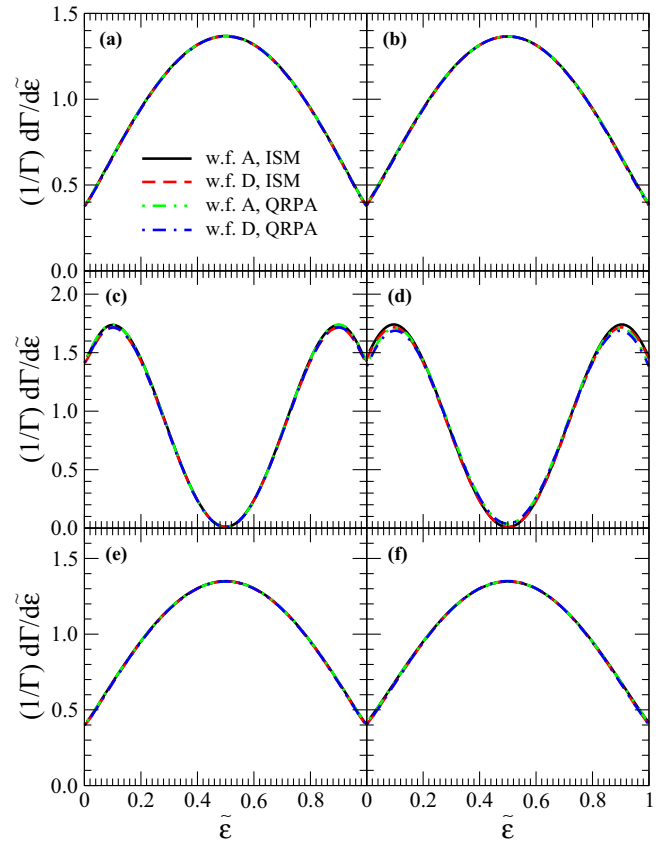

FIG. 6. (Color online) The single-electron differential decay rate normalized to the total decay rate vs the electron energy $\tilde{\varepsilon}$ [$\tilde{\varepsilon} = (\varepsilon - m_e)/Q_{\beta\beta}$] for $0\nu\beta\beta$ decay of ^{76}Ge [left panels (a), (c), and (e)] and ^{136}Xe [right panels (b), (d), and (f)]. Results are presented for mechanism determined by factors $|m_{\beta\beta}|^2$ ($\langle\lambda\rangle = \langle\eta\rangle = 0$) [panels (e) and (f)], $|\langle\lambda\rangle|^2$ ($m_{\beta\beta} = \langle\eta\rangle = 0$) [panels (c) and (d)], and $|\langle\eta\rangle|^2$ ($m_{\beta\beta} = \langle\lambda\rangle = 0$) [panels (e) and (f)]. Approximate electron wave functions (w.f. A) and exact Dirac wave functions with finite nuclear size and electron screening (w.f. D) are considered. Nuclear matrix elements calculated within the ISM [23] and the QRPA [22] are used in calculations.

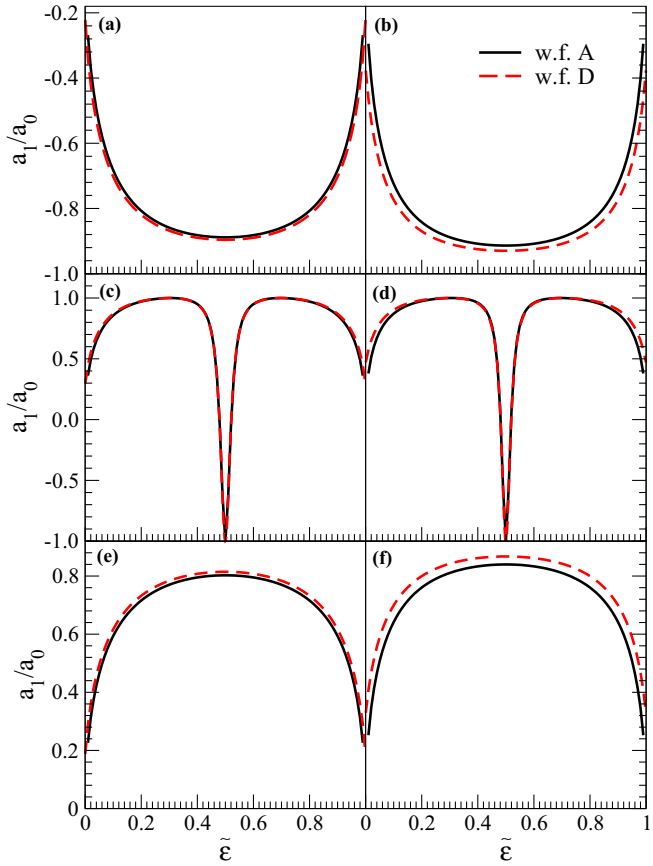

FIG. 7. (Color online) The angular correlation factor [see Eq. (55)] vs the electron energy $\tilde{\varepsilon}$ [$\tilde{\varepsilon} = (\varepsilon - m_e)/Q_{\beta\beta}$] for $0\nu\beta\beta$ decay of ^{76}Ge [left panels (a), (c), and (e)] and ^{136}Xe [right panels (b), (d), and (f)]. Results are presented for mechanism determined by factors $|m_{\beta\beta}|^2$ ($\langle\lambda\rangle = \langle\eta\rangle = 0$) [panels (e) and (f)], $|\langle\lambda\rangle|^2$ ($m_{\beta\beta} = \langle\eta\rangle = 0$) [panels (c) and (d)], and $|\langle\eta\rangle|^2$ ($m_{\beta\beta} = \langle\lambda\rangle = 0$) [panels (e) and (f)]. Approximate electron wave functions (w.f. A) and exact Dirac wave functions with finite nuclear size and electron screening (w.f. D) are considered. Nuclear matrix elements calculated within the ISM [23] are used in calculations.

(i) Case $m_{\beta\beta} \neq 0$ ($\langle\lambda\rangle = 0$ and $\langle\eta\rangle = 0$):

$$d\Gamma = g_A^4 |M_{GT}|^2 \left(\frac{|m_{\beta\beta}|}{m_e}\right)^2 dC_{mm}. \quad (51)$$

(ii) Case $\langle\lambda\rangle \neq 0$ ($m_{\beta\beta} = 0$ and $\langle\eta\rangle = 0$):

$$d\Gamma = g_A^4 |M_{GT}|^2 \langle\lambda\rangle^2 dC_{\lambda\lambda}. \quad (52)$$

(iii) Case $\langle\eta\rangle \neq 0$ ($m_{\beta\beta} = 0$ and $\langle\lambda\rangle = 0$):

$$d\Gamma = g_A^4 |M_{GT}|^2 \langle\eta\rangle^2 dC_{\eta\eta}, \quad (53)$$

where

$$\begin{aligned} dC_{mm} &= (1-\chi_F)^2 d\mathcal{G}_{01}, \\ dC_{\lambda\lambda} &= \chi_{2-}^2 d\mathcal{G}_{02} + \tfrac{1}{9}\chi_{1+}^2 d\mathcal{G}_{011} - \tfrac{2}{9}\chi_{1+}\chi_{2-} d\mathcal{G}_{010}, \\ dC_{\eta\eta} &= \chi_{2+}^2 d\mathcal{G}_{02} + \tfrac{1}{9}\chi_{1-}^2 d\mathcal{G}_{011} - \tfrac{2}{9}\chi_{1-}\chi_{2+} d\mathcal{G}_{010} \\ &\quad + \chi_P^2 d\mathcal{G}_{08} - \chi_P \chi_R d\mathcal{G}_{07} + \chi_R^2 d\mathcal{G}_{09}, \end{aligned} \quad (54)$$

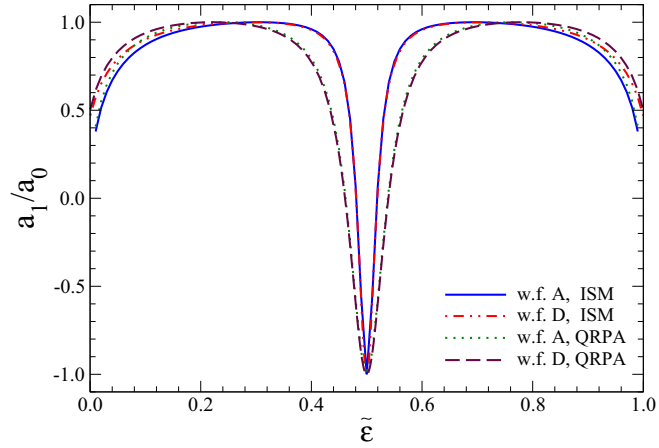

FIG. 8. (Color online) The angular correlation factor [see Eq. (55)] vs the electron energy $\tilde{\varepsilon}$ [$\tilde{\varepsilon} = (\varepsilon - m_e)/Q_{\beta\beta}$] for $0\nu\beta\beta$ decay of ^{136}Xe. Results are presented for the $|\langle\lambda\rangle|^2$ term ($m_{\beta\beta} = \langle\eta\rangle = 0$). Approximate electron wave functions (w.f. A) and exact Dirac wave functions with finite nuclear size and electron screening (w.f. D) are considered. Nuclear matrix elements calculated within the ISM [23] and the QRPA [22] are used in calculations.

with

$$\begin{aligned} d\mathcal{G}_{0k} &= d\cos\theta d\tilde{\varepsilon}_1 \frac{G_\beta^4 m_e^2 Q_{\beta\beta}}{64\pi^5 R^2} (h_{0k}(\varepsilon_1,\varepsilon_2,R)\cos\theta \\ &\quad + g_{0k}(\varepsilon_1,\varepsilon_2,R)) p_1 p_2 \varepsilon_1 \varepsilon_2 \\ &\equiv a_0^k + a_1^k \cos\theta, \quad k = 1,2,\ldots,11. \end{aligned} \quad (55)$$

Here, a_0^k and a_1^k are angular correlation coefficients. $\mathcal{G}_{0k} = \ln 2 G_{0k}$.

The differential decay rate can be written as

$$\frac{d\Gamma}{d\cos\theta\, d\tilde{\varepsilon}_1} = a_0(1 + a_1/a_0 \cos\theta). \quad (56)$$

Here a_1/a_0 is the energy-dependent angular correlation coefficient, which depends also on the chosen limiting case for lepton number violating parameters.

In Fig. 6 the single-electron spectra normalized to the total decay rate are shown as function of the electron energy $\tilde{\varepsilon}$ for the $0\nu\beta\beta$ decay of ^{76}Ge and ^{136}Xe due to nonvanishing $m_{\beta\beta}$, $\langle\lambda\rangle$, and $\langle\eta\rangle$. This quantity, ideally accessible experimentally, depends only very weakly on the chosen isotope, the set of calculated nuclear matrix elements, and whether a standard or improved description of electron wave functions is used. The different characteristics of these three limiting cases provide a possibility to identify which of the parameters is responsible for $0\nu\beta\beta$ decay.

In Fig. 7 the angular correlation factors a_1/a_0 are presented as a function of the electron energy $\tilde{\varepsilon}$ for the $0\nu\beta\beta$ decay of ^{76}Ge and ^{136}Xe due to nonvanishing $m_{\beta\beta}$, $\langle\lambda\rangle$, and $\langle\eta\rangle$. The ISM nuclear matrix elements are considered. The results slightly depends on the type of electron wave functions and manifest similar behavior for both isotopes. In Fig. 8 the a_1/a_0 behavior in detail for the $\langle\lambda\rangle$ limiting case is shown. Note that results in this case are affected more significantly by the choice of nuclear matrix elements and that the choice of electron

wave functions changes a_1/a_0 only slightly for small and large values of electron energy.

VII. SUMMARY AND CONCLUSIONS

It is often assumed that if and when the neutrinoless double beta decay ($0\nu\beta\beta$) is observed, it will be caused by the exchange of a virtual light Majorana neutrino and its decay rate will be proportional to the square of the effective Majorana mass $m_{\beta\beta}$. It would be possible, therefore, to constrain or determine the magnitude of this fundamental parameter based on experimental limits or values of the decay half-life. However, that is not the only possibility. Many other manifestations of the "physics beyond the standard model" that would cause the $0\nu\beta\beta$ decay were considered in the past. Among them the possibility of the right-handed lepton and/or hadron currents that could perhaps compete with the mass mechanism was often discussed; see e.g. [6,7]. Such a possibility arises naturally in the left-right symmetric models. In that case the $0\nu\beta\beta$-decay half-life will depend not only on the $m_{\beta\beta}$ but also, perhaps dominantly, on the parameters that characterize the right-handed currents, denoted $\langle\lambda\rangle$ and $\langle\eta\rangle$ here.

When it is assumed that the right-handed currents exist, the $0\nu\beta\beta$-decay half-life can be expressed as a sum of products of the phase-space factors, nuclear matrix elements, and the fundamental parameters that characterize the new physics. In this work the particular emphasis is on the reformulation of this relation, on a careful derivation of all terms in that expression, and on the new and more general evaluation of the phase-space factors. The phase-space factors depend on the wave functions of the emitted electrons, and various approximations were used in the past in their calculation. We use here the exact solutions of the Dirac equation for the $s_{1/2}$ and $p_{1/2}$ electron states, solving the Dirac equation in the potential that includes the nuclear finite size and the electron screening. The possible approximations to this problem are analyzed and discussed, and in particular it is shown that using just the first-order expansion in r, in order to include the nuclear finite size with the sufficient accuracy, is not enough. A complete table of accurate phase-space factors for nuclei of interest is given. Compared with the treatment that uses only the first terms in the r expansion (denoted as approximation A in this work), the exact phase-space factors (approximation D) are smaller, in particular in the heavier nuclei (^{130}Te and ^{150}Nd) the reduction is ∼30% or even more.

It is also often assumed that the nucleons involved in the $0\nu\beta\beta$ decay are essentially at the nuclear surface, hence the phase-space factors are evaluated with the electrons placed at $r = R$. The adequacy of that assumption was not tested until now. Here it is shown—see Fig. 3 and Table II—that it is a reasonable assumption, even though an increase in the phase-space factors by a few percent in the heavier candidate nuclei is expected.

Having the full set of the phase-space factors, it is possible by combining them with the full set of nuclear matrix elements evaluated elsewhere, to obtain simultaneous or separate limits for the fundamental parameters $m_{\beta\beta}$ and those associated with the right-handed currents $\langle\lambda\rangle$ and $\langle\eta\rangle$. It turns out that again the difference between the previously used approximation A (just the first term in the expansion in r) and the more exact treatment (exact Dirac electron wave functions with the nuclear radius R and electron screening) in the final limits is relatively benign in ^{76}Ge, enlarging the limits on the fundamental parameters only by about 5%. However, in the heavier nucleus ^{136}Xe the effect is larger, 10–15%.

It is well known that by convincingly determining the $0\nu\beta\beta$ half-life one would obviously show that the total lepton number is not a conserved quantity. However, that determination by itself will be insufficient to decide which of the possible mechanisms is responsible for the decay. If, in addition, the single-electron energy spectra, and the angular distribution of the emitted electrons, could be detected, it will help substantially in that task. If one of the possible parameters $m_{\beta\beta}$, $\langle\lambda\rangle$, or $\langle\eta\rangle$ dominates, the single-particle spectra and angular correlations will be a decisive tool to determine the mechanism. Formulas that determine these quantities and the corresponding phase-space factors are shown here. In that case the exact treatment of nuclear size makes only little difference.

ACKNOWLEDGMENTS

This work is supported in part by the VEGA Grant Agency of the Slovak Republic under Contract No. 1/0876/12, by Slovak Research and Development Agency under Contract No. APVV-14-0524, and by the Ministry of Education, Youth and Sports of the Czech Republic under Contract No. LM2011027.

[1] J. Schechter and J. W. F. Valle, Phys. Rev. D **25**, 2951 (1982).
[2] J. D. Vergados, H. Ejiri, and F. Šimkovic, Rep. Prog. Phys. **75**, 106301 (2012).
[3] J. Kotila and F. Iachello, Phys. Rev. C **85**, 034316 (2012).
[4] J. C. Pati and A. Salam, Phys. Rev. D **10**, 275 (1974); R. Mohapatra and J. C. Pati, *ibid.* **11**, 2558 (1975).
[5] G. Senjanovic and R. N. Mohapatra, Phys. Rev. D **12**, 1502 (1975); R. N. Mohapatra and G. Senjanovic, Phys. Rev. Lett. **44**, 912 (1980); Phys. Rev. D **23**, 165 (1981).
[6] M. Doi, T. Kotani, and E. Takasugi, Prog. Theor. Phys. Suppl. **83**, 1 (1985).
[7] T. Tomoda, Rep. Prog. Phys. **54**, 53 (1991).
[8] V. Tello, M. Nemevšek, F. Nesti, G. Senjanović, and F. Vissani, Phys. Rev. Lett. **106**, 151801 (2011).
[9] M. Nemevšek, F. Nesti, G. Senjanović, and V. Tello, arXiv:1112.3061.
[10] J. Barry and W. Reodejohann, J. High Energy Phys. 09 (2013) 153.
[11] P. S. Bhupal Dev, S. Goswami, and M. Mitra, Phys. Rev. D **91**, 113004 (2015).
[12] F. F. Deppisch, J. Harz, W.-C. Huang, M. Hirsch, and H. Päs, Phys. Rev. D **92**, 036005 (2015).
[13] M. E. Rose, *Relativistic Electron Theory* (John Wiley and Sons, New York, 1961).
[14] V. B. Beresteckij, E. M. Lifshitz, and L. P. Pitaevskij, *Quantum Electrodynamics*, Vol. IV (Nauka, Moscow, 1989).

[15] F. Salvat, J. M. Fernandez-Varea, and W. Williamson, Jr., Comput. Phys. Commun. **90**, 151 (1995).
[16] S. Esposito, Am. J. Phys. **70**, 852 (2002).
[17] Z.-Z. Xing, Phys. Rev. D **85**, 013008 (2012).
[18] D. Štefánik, R. Dvornický, and F. Šimkovic, in *Proceedings of the 33rd International Workshop on Nuclear Theory (IWNT-33), Rila Mountains*, edited by A. Georgieva and N. Minkov (Heron Press Ltd., Sofia, Bulgaria, 2014), Vol. 33, pp. 115–121.
[19] G. L. Fogli, E. Lisi, A. Marrone, D. Montanino, A. Palazzo, and A. M. Rotunno, Phys. Rev. D **86**, 013012 (2012).
[20] F. Šimkovic, G. Pantis, J. D. Vergados, and A. Faessler, Phys. Rev. C **60**, 055502 (1999).
[21] F. Šimkovic, V. Rodin, A. Faessler, and P. Vogel, Phys. Rev. C **87**, 045501 (2013).
[22] K. Muto, E. Bender, and H. V. Klapdor, Z. Phys. A **334**, 187 (1989).
[23] E. Caurier, F. Nowacki, A. Poves, and J. Retamosa, Phys. Rev. Lett. **77**, 1954 (1996).
[24] E. Caurier, F. Nowacki, and A. Poves, Eur. Phys. J. A **36**, 195 (2008).
[25] M. Agostini *et al.* (GERDA Collaboration), Phys. Rev. Lett. **111**, 122503 (2013).
[26] A. Gando *et al.* (KamLAND-Zen Collabboration), Phys. Rev. Lett. **110**, 062502 (2013); M. Auger *et al.* (EXO Collaboration), *ibid.* **109**, 032505 (2012).
[27] R. Arnold *et al.* (SuperNEMO Collaboration), Eur. Phys. J. C **70**, 927 (2010).
[28] V. Alvarez *et al.* (NEXT Collaboration), arXiv:1106.3630.